 CMES, vol.58, no.1, pp.75-108, 2010

Locking-free Thick-Thin Rod/Beam Element for Large Deformation Analyses of Space-Frame Structures, Based on the Reissner Variational Principle and A Von Karman Type Nonlinear Theory

Y.C. Cai[1,2], J.K. Paik[3] and S.N. Atluri[4]

Abstract: This paper presents a new shear flexible beam/rod element for large deformation analyses of space-frame structures comprising of thin or thick members, based on the Reissner variational principle and a von Karman type nonlinear theory of deformation in the co-rotational reference frame of the present beam element. The C^0 continuous trial functions for transverse rotations in two independent directions are used over each element, to derive an explicit expression for the (16x16) *symmetric* tangent stiffness matrix of the beam element in the co-rotational reference frame. When compared to the primal approach wherein C^1 continuous trial functions for transverse displacements over each element are necessary, the trial functions for the transverse bending moments, shear deformations and rotations are very simple in the current approach, and can be assumed to be linear within each element. The present (16×16) symmetric tangent stiffness matrices of the thick/thin beam are much simpler than those of many others in the literature. Numerical examples demonstrate that the present element is free from shear locking in the thin beam limit, and is suitable for the large deformation analysis of spaced frames with thick/thin members. The present methodologies can be extended to study the very large deformations of plates and shells as well.

Keywords: Large deformation, Unsymmetrical cross-section, Thick Beam/Rod, Locking-free, Explicit tangent stiffness, Space frames, Reissner variational principle

[1] Key Laboratory of Geotechnical and Underground Engineering of Ministry of Education, Department of Geotechnical Engineering, Tongji University, Shanghai 200092, P.R.China. E-mail:yc_cai@163.net

[2] Key Laboratory for the Exploitation of Southwest Resources and Environmental Disaster Control Engineering, Ministry of Education, Chongqing University, Chongqing 400044, P.R.China

[3] The Lloyd's Register Educational Trust (The LRET) Research Center of Excellence, Pusan National University, Korea

[4] Center for Aerospace Research & Education, University of California, Irvine

1 Introduction

Exact and efficient nonlinear large deformation analyses of space frames have attracted much attention due to their significance in diverse engineering applications, such as civil and aerospace engineering, and tensegrity structures in biological applications. In the past decades, many different methods were developed by numerous researchers for the geometrically nonlinear analyses of 3D frame structures. Bathe and Bolourchi (1979) employed the total Lagrangian and updated Lagrangian approaches to formulate fully nonlinear 3D continuum beam elements. Punch and Atluri (1984) examined the performance of linear and quadratic Serendipity hybrid-stress 2D and 3D beam elements. Based on geometric considerations, Lo (1992) developed a general 3D nonlinear beam element, which can remove the restriction of small nodal rotations between two successive load increments. Kondoh, Tanaka and Atluri (1986), Kondoh and Atluri (1987), Shi and Atluri(1988) presented the derivations of explicit expressions of the tangent stiffness matrix, without employing either numerical or symbolic integration. Zhou and Chan (2004a, 2004b) developed a precise element capable of modeling elastoplastic buckling of a column by using a single element per member for large deflection analysis. Izzuddin (2001) clarified some of the conceptual issues which are related to the geometrically nonlinear analysis of 3D framed structures. Simo (1985), Mata, Oller and Barbat (2007, 2008), Auricchio, Carotenuto and Reali (2008) considered the nonlinear constitutive behavior in the geometrically nonlinear formulation for beams. Iura and Atluri (1988), Chan (1994), Xue and Meek (2001), Wu, Tsai and Lee(2009) studied the nonlinear dynamic response of the 3D frames. Lee, Lin, Lee, Lu and Liu (2008), Lee, Lu, Liu and Huang (2008), Lee and Wu (2009) gave the exact large deflection solutions of the beams for some special cases. Gendy and Saleeb (1992); Atluri, Iura, and Vasudevan(2001) had brief discussions of arbitrary cross sections. Atluri and Zhu (1998), Zhu, Zhang and Atluri (1999), Wen and Hon (2007); Dinis, Jorge and Belinha (2009), Han, Rajendran and Atluri (2005), Lee and Chen (2009) applied meshless methods to the analyses of nonlinear problems with large deformations or rotations. Gendy and Saleeb (1992), Atluri, Iura, and Vasudevan(2001) had brief discussions of the frames with arbitrary cross sections. Large rotations in beams, plates and shells, and attendant variational principles involving the rotation tensor as a direct variable, were studied extensively by Atluri and his co-workers (see, for instance, Atluri 1980, Atluri 1984 ,and Atluri and Cazzani 1994).

In previous papers (Cai, Paik and Atluri 2009a,b), we proposed two types of simple "thin" beam/rod elements, based on simple mechanics and physical clarity, for geometrically nonlinear large rotation analyses of space frames consisting of members of arbitrary cross-section. However, the elements are only accurate for very thin beams and for structures containing thin beams, because the influence of the

shear deformation was neglected. The neglect of the effect of the shear deformation may impair the computational accuracy and may lead to the error of results for moderately thick structures. Researchers had developed many shear-flexible beam elements (Reddy 1997; Mukherjee and Prathap 2001; Atluri, Cho and Kim 1999; Zhang and Di 2003; Li 2007) to obtain acceptable results for a wide range of element thicknesses, and successfully applied them to diverse engineering fields. Nevertheless, these methods will involve very complex algebraic derivations when they are extended to the large deformation analysis of structures. In this paper, we present a new shear flexible beam/rod element for large deformation analyses of space-frame structures consisting of thick or thin members, based on the Reissner variational principle and a von Karman type nonlinear theory of deformation in the co-rotational reference frame of the present beam element. The C^0 continuous trial functions for transverse rotations in two independent directions, over each element, are used to derive an explicit expression for the (16x16) *symmetric* tangent stiffness matrix of the beam element in the co-rotational reference frame. When compared to the primal approach wherein C^1 continuous trial functions for transverse displacements over each element are necessary (Zhu, Cai, Paik and Atluri 2010), the trial functions for the transverse bending moments, shear deformations and rotations are very simple in the current approach, and can be assumed to be linear within each element. The present (16×16) *symmetric* tangent stiffness matrices (which remain symmetric throughout the deformations and large rotations) of the beam, based on the Reissner variational principle and the von Karman type simplified rod theory, are much simpler than those of many others in the literature, such as, Simo (1985), Bathe and Bolourchi (1979), Crisfield (1990), Kondoh, Tanaka and Atluri (1986), Kondoh and Atluri (1987), and Shi and Atluri (1988). Numerical examples demonstrated that the present element is free from shear locking and is suitable for the large deformation analysis of spaced frames consisting of thick or thin members. The present methodologies can be extended to study the very large deformations of plates and shells (Sladek, Sladek, Solek and Atluri 2008; Majorana and Salomoni 2008; Gato and Shie 2008; Kulikov and Plotnikova 2008) as well.

2 Von-Karman type nonlinear theory including shear deformation for a rod with large deformations

We consider a fixed global reference frame with axes $\bar{x}_i\,(i=1,2,3)$ and base vectors $\bar{\mathbf{e}}_i$. An initially straight rod of an arbitrary cross-section and base vectors $\tilde{\mathbf{e}}_i$, in its undeformed state, with local coordinates $\tilde{x}_i\,(i=1,2,3)$, is located arbitrarily in space, as shown in Fig.1. The current configuration of the rod, after arbitrarily large deformations (but small strains) is also shown in Fig.1.

The local coordinates in the reference frame in the current configuration are x_i and

the base vectors are $\mathbf{e}_i\,(i=1,2,3)$. The nodes 1 and 2 of the rod (or an element of the rod) are supposed to undergo arbitrarily large displacements, and the rotations between the $\tilde{\mathbf{e}}_i\,(i=1,2,3)$ and the $\mathbf{e}_k\,(k=1,2,3)$ base vectors are assumed to be arbitrarily finite. In the continuing deformation from the current configuration, the local displacements in the $x_i\,(\mathbf{e}_i)$ coordinate system are assumed to be moderate, and the local gradient $(\partial u_{10}/\partial x_1)$ is assumed to be small compared to the transverse rotations $(\partial u_{\alpha 0}/\partial x_1)\,(\alpha=2,3)$. Thus, in essence, a von-Karman type deformation is assumed for the continued deformation from the current configuration, in the co-rotational frame of reference $\mathbf{e}_i\,(i=1,2,3)$ in the local coordinates $x_i\,(i=1,2,3)$. If H is the characteristic dimension of the cross-section of the rod, the precise assumptions governing the continued deformations from the current configuration are

$\frac{u_{10}}{H}\leq 1;\ \frac{H}{L}$ need not be ≤ 1.

$$\frac{u_{\alpha 0}}{H}\approx \mathrm{O}\,(1)\ \ (\alpha=2,3)$$

$$\frac{\partial u_{10}}{\partial x_1}<<\frac{\partial u_{\alpha 0}}{\partial x_1}\ \ (\alpha=2,3)$$

and $\left(\frac{\partial u_{\alpha 0}}{\partial x_1}\right)^2\ \ (\alpha=2,3)$ are not negligible.

As shown in Fig.2, we consider the large deformations of a cylindrical rod, subjected to bending (in two directions), and torsion around x_1. The cross-section is unsymmetrical around x_2 and x_3 axes,and is constant along x_1.

As shown in Fig.2, the warping displacement due to the torque T around x_1 axis is $u_{1T}\,(x_2,x_3)$ and does not depend on x_1, the axial displacement at the origin ($x_2=x_3=0$) is $u_{10}\,(x_1)$, and the bending displacement at $x_2=x_3=0$ along the axis x_1 are $u_{20}\,(x_1)$ (along x_2) and $u_{30}\,(x_1)$ (along x_3).

We consider only loading situations when the generally 3-dimensional displacement state in the $\mathbf{e}_i$ system, donated as

$$u_i=u_i\,(x_k)\ \ i=1,2,3;\ k=1,2,3$$

is simplified to be of the type:

$$\begin{aligned} u_1&=u_{1T}\,(x_2,x_3)+u_{10}\,(x_1)-x_2\theta_2-x_3\theta_3\\ u_2&=u_{20}\,(x_1)-\theta_1 x_3\\ u_3&=u_{30}\,(x_1)+\theta_1 x_2 \end{aligned}\qquad (1)$$

where θ_1 is the total torsion of the rod at x_1 due to the torque T, θ_2 is the total rotation around x_3, and θ_3 is the total rotation around x_2, where θ_2 and θ_3 include the influence of the shear deformation.

2.1 Strain-displacement relations

Considering only von Karman type nonlinearities in the rotated reference frame $\mathbf{e}_i(x_i)$, we can write the Green-Lagrange strain-displacement relations in the updated Lagrangian co-rotational frame $\mathbf{e}_i$ in Fig.1 as:

$$\begin{aligned}
\varepsilon_{11} &= \frac{\partial u_1}{\partial x_1} + \frac{1}{2}\left(\frac{\partial u_2}{\partial x_1}\right)^2 + \frac{1}{2}\left(\frac{\partial u_3}{\partial x_1}\right)^2 \\
&= \frac{\partial u_{10}}{\partial x_1} + \frac{1}{2}\left(\frac{\partial u_{20}}{\partial x_1}\right)^2 + \frac{1}{2}\left(\frac{\partial u_{30}}{\partial x_1}\right)^2 - x_2\frac{\partial \theta_2}{\partial x_1} - x_3\frac{\partial \theta_3}{\partial x_1} \\
\varepsilon_{12} &= \frac{1}{2}\left(\frac{\partial u_1}{\partial x_2} + \frac{\partial u_2}{\partial x_1}\right) = \frac{1}{2}\left(\frac{\partial u_{1T}}{\partial x_2} - \frac{\partial \theta_1}{\partial x_1}\, x_3 + \frac{\partial u_{20}}{\partial x_1} - \theta_2\right) \\
\varepsilon_{13} &= \frac{1}{2}\left(\frac{\partial u_1}{\partial x_3} + \frac{\partial u_3}{\partial x_1}\right) = \frac{1}{2}\left(\frac{\partial u_{1T}}{\partial x_3} + \frac{\partial \theta_1}{\partial x_1}\, x_2 + \frac{\partial u_{30}}{\partial x_1} - \theta_3\right) \\
\varepsilon_{22} &= \frac{\partial u_2}{\partial x_2} + \frac{1}{2}\left(\frac{\partial u_1}{\partial x_2}\right)^2 + \frac{1}{2}\left(\frac{\partial u_2}{\partial x_2}\right)^2 + \frac{1}{2}\left(\frac{\partial u_3}{\partial x_2}\right)^2 \approx 0 \\
\varepsilon_{23} &\approx 0 \\
\varepsilon_{33} &\approx 0
\end{aligned} \tag{2}$$

By letting

$$\begin{aligned}
\theta_1' &= \theta_{1,1} \\
\gamma_2 &= u_{20,1} - \theta_2 \\
\gamma_3 &= u_{30,1} - \theta_3 \\
\chi_{22} &= -u_{20,11} \\
\chi_{33} &= -u_{30,11} \\
\varepsilon_{11}^0 &= u_{10,1} + \frac{1}{2}(u_{20,1})^2 + \frac{1}{2}(u_{30,1})^2 = \varepsilon_{11}^{0L} + \varepsilon_{11}^{0N}
\end{aligned} \tag{3}$$

the strain-displacement relations can be rewritten as

$$\begin{aligned}
\varepsilon_{11} &= \varepsilon_{11}^0 + x_2\chi_{22} + x_3\chi_{33} + x_2\gamma_{2,1} + x_3\gamma_{3,1} \\
\varepsilon_{12} &= \frac{1}{2}\left(u_{1T,2} - \theta_1'\, x_3 + \gamma_2\right) \\
\varepsilon_{13} &= \frac{1}{2}\left(u_{1T,3} + \theta_1'\, x_2 + \gamma_3\right) \\
\varepsilon_{22} &= \varepsilon_{33} = \varepsilon_{23} = 0
\end{aligned} \tag{4}$$

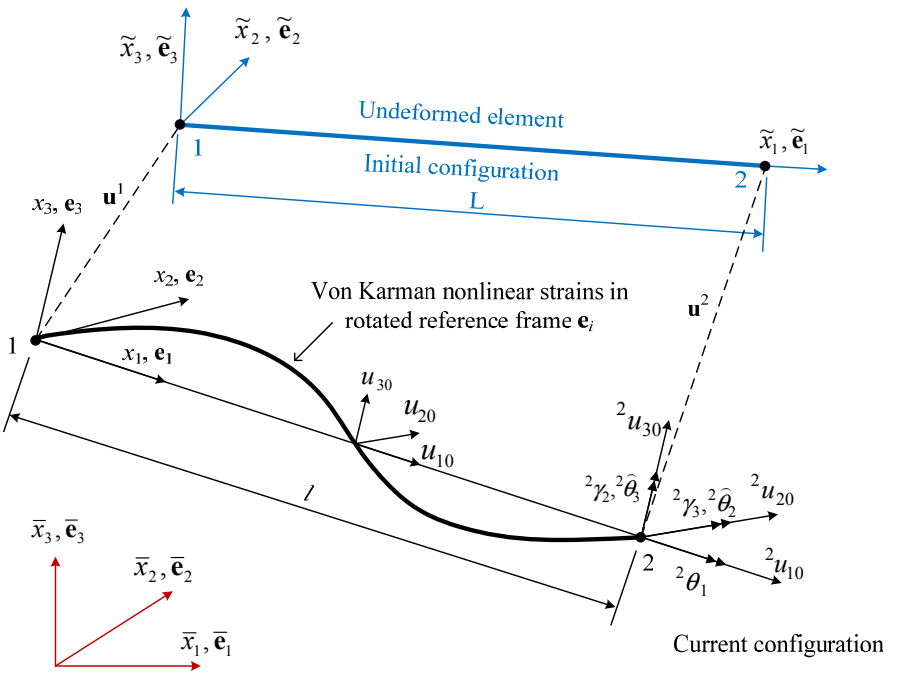

Figure 1: Kinematics of deformation of a space framed member

where $,i$ denotes a differentiation with respect to x_i.

The matrix form of the Eq.(4) is

$$\boldsymbol{\varepsilon} = \boldsymbol{\varepsilon}^{Lb} + \varepsilon^{Ls} + \boldsymbol{\varepsilon}^{N} = \boldsymbol{\varepsilon}^{L} + \boldsymbol{\varepsilon}^{N} \tag{5}$$

where $\boldsymbol{\varepsilon}^{Lb}$ is the linear part of the bending strain, $\boldsymbol{\varepsilon}^{N}$ is the nonlinear part of the bending strain, $\boldsymbol{\varepsilon}^{Ls}$ is the shear strain, and

$$\boldsymbol{\varepsilon}^{Lb} = \begin{Bmatrix} \varepsilon_{11}^{Lb} \\ \varepsilon_{12}^{Lb} \\ \varepsilon_{13}^{Lb} \end{Bmatrix} = \begin{Bmatrix} u_{10,1} + x_2\chi_{22} + x_3\chi_{33} \\ \frac{1}{2}\left(u_{1T,2} - \theta_1' \, x_3\right) \\ \frac{1}{2}\left(u_{1T,3} + \theta_1' \, x_2\right) \end{Bmatrix} \tag{6}$$

$$\boldsymbol{\varepsilon}^{Ls} = \begin{Bmatrix} \varepsilon_{11}^{Ls} \\ \varepsilon_{12}^{Ls} \\ \varepsilon_{13}^{Ls} \end{Bmatrix} = \begin{Bmatrix} x_2\gamma_{2,1} + x_3\gamma_{3,1} \\ \gamma_2/2 \\ \gamma_3/2 \end{Bmatrix} \tag{7}$$

$$\boldsymbol{\varepsilon}^{N} = \begin{Bmatrix} \varepsilon_{11}^{N} \\ \varepsilon_{12}^{N} \\ \varepsilon_{13}^{N} \end{Bmatrix} = \begin{Bmatrix} \frac{1}{2}\left(u_{20,1}\right)^2 + \frac{1}{2}\left(u_{30,1}\right)^2 \\ 0 \\ 0 \end{Bmatrix} \tag{8}$$

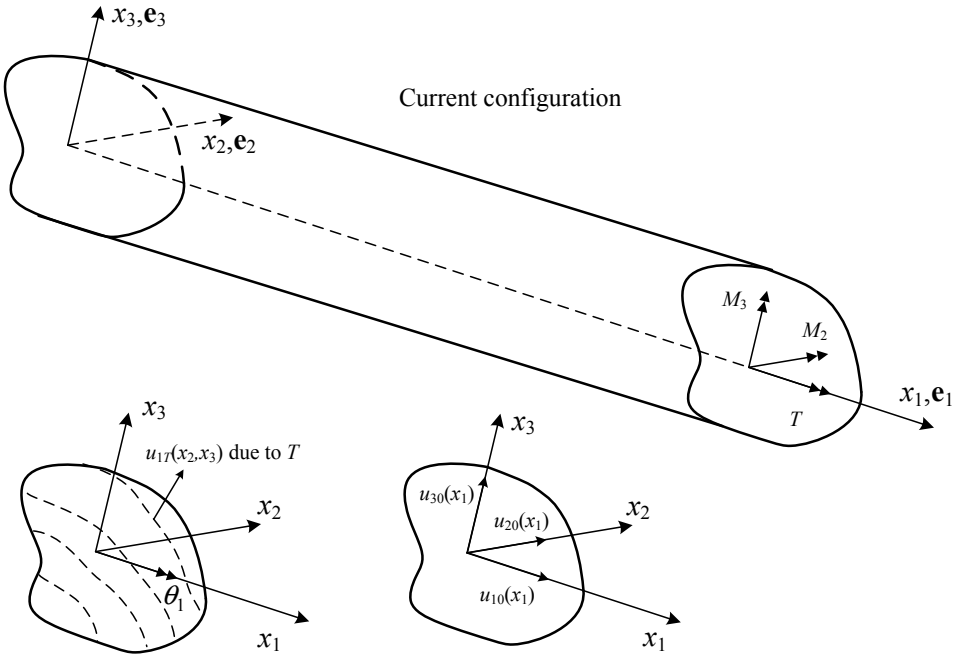

Figure 2: Large deformation analysis model of a cylindrical rod

From Eqs.(3) and (4), it is seen that in the present formulation, the transverse displacements (u_{20} and u_{30}) as well as the transverse shear strains (γ_2 and γ_3) are retained as independent variables. This type of formulation has beem clearly shown (Atluri 2005) to lead to be locking-free and remains uniformly valid for either thick or thin beams, without using such numerical gimmicks as selective/reduced integrations and without the need for stabilizing the attendant spurious modes of zero-energy. On the other hand, one may also use formulations wherein the transverse displacements (u_{20} and u_{30}) as well as the total rotations (θ_2 and θ_3) are retained as independent variables. However, it has been simply explained in (Atluri 2005), how such formulations lead to locking, thus necessitating the use of selective reduced integration and the need for the stabilization of the attendant zero-energy modes.

2.2 Stress-Strain relations

Taking the material to be linear elastic, we assume that the additional second Piola-Kirchhoff stress, denoted by tensor $\mathbf{S}^1$ in the updated Lagrangian co-rotational reference frame $\mathbf{e}_i$ of Fig.1 (in addition to the pre-existing Cauchy stress due to prior

deformation, denoted by $\boldsymbol{\tau}^0$), is given by:

$$\begin{aligned} S_{11}^1 &= E\varepsilon_{11} \\ S_{12}^1 &= 2\mu\varepsilon_{12} \\ S_{13}^1 &= 2\mu\varepsilon_{13} \\ S_{22}^1 &= S_{33}^1 = S_{23}^1 \approx 0 \end{aligned} \tag{9}$$

where $\mu = \frac{E}{2(1+\nu)}$; E is the elastic modulus; ν is the Poisson ratio.
By using Eq.(5), Eq.(9) can also be written as

$$\mathbf{S}^1 = \tilde{\mathbf{D}}\left(\boldsymbol{\varepsilon}^{Lb} + \boldsymbol{\varepsilon}^{Ls} + \boldsymbol{\varepsilon}^{N}\right) = \mathbf{S}^{Lb} + \mathbf{S}^{Ls} + \mathbf{S}^{N} = \mathbf{S}^{1L} + \mathbf{S}^{1N} \tag{10}$$

where

$$\tilde{\mathbf{D}} = \begin{bmatrix} E & 0 & 0 \\ 0 & 2\mu & 0 \\ 0 & 0 & 2\mu \end{bmatrix} \tag{11}$$

From Eq.(4) and Eq.(9), the generalized nodal forces of the rod element in Fig.1 can be written as

$$\begin{aligned} N_{11} &= \int_A S_{11}^1 dA \\ &= E\left(A\varepsilon_{11}^0 + \chi_{22}\int_A x_2 dA + \chi_{33}\int_A x_3 dA + \gamma_{2,1}\int_A x_2 dA + \gamma_{3,1}\int_A x_3 dA\right) \\ &= E\left(A\varepsilon_{11}^0 + I_2\chi_{22} + I_3\chi_{33} + I_2\gamma_{2,1} + I_3\gamma_{3,1}\right) \\ M_{33} &= \int_A S_{11}^1 x_3 dA = E\int_A \left(\varepsilon_{11}^0 + x_2\chi_{22} + x_3\chi_{33} + x_2\gamma_{2,1} + x_3\gamma_{3,1}\right)x_3 dA \\ &= E\left(I_3\varepsilon_{11}^0 + I_{23}\chi_{22} + I_{33}\chi_{33} + I_{23}\gamma_{2,1} + I_{33}\gamma_{3,1}\right) \\ M_{22} &= \int_A S_{11}^1 x_2 dA = E\int_A \left(\varepsilon_{11}^0 + x_2\chi_{22} + x_3\chi_{33} + x_2\gamma_{2,1} + x_3\gamma_{3,1}\right)x_2 dA \\ &= E\left(I_2\varepsilon_{11}^0 + I_{22}\chi_{22} + I_{23}\chi_{33} + I_{22}\gamma_{2,1} + I_{23}\gamma_{3,1}\right) \\ T &= \int_A S_{13}^1 x_2 - S_{12}^1 x_3 dA = 2\mu\int_A (x_2\varepsilon_{13} - x_3\varepsilon_{12}) dA \\ &= \frac{2\mu}{2}\int_A \left[\left(u_{1T,3} + \theta_1' x_2 + \gamma_3\right)x_2 - \left(u_{1T,2} - \theta_1' x_3 + \gamma_2\right)x_3\right] dA \\ &= \mu\int_A \theta_1'\left(x_2^2 + x_3^2\right) dA + \mu\int_A \left(\gamma_3 x_2 - \gamma_2 x_3\right) dA + \mu\int_A \left(u_{1T,3}x_2 - u_{1T,2}x_3\right) dA \\ &= \mu I_{rr}\theta_1' + \mu I_2\gamma_3 - \mu I_3\gamma_2 + \mu\oint_S \left(u_{1T}n_3 x_2 - u_{1T}n_2 x_3\right) dS \\ &= \mu I_{rr}\theta_1' + \mu I_2\gamma_3 - \mu I_3\gamma_2 \end{aligned}$$

$$Q_{12} = \int_A S_{12}^1 dA = \mu \int_A \left(u_{1T,2} - \theta_1' x_3 + \gamma_2\right) dA \approx \mu \left(-I_3 \theta_1' + A\gamma_2\right)$$
$$Q_{13} = \int_A S_{13}^1 dA = \mu \int_A \left(u_{1T,3} + \theta_1' x_2 + \gamma_3\right) dA \approx \mu \left(I_2 \theta_1' + A\gamma_3\right) \tag{12}$$

where n_j is the outward normal, $I_2 = \int_A x_2 dA$, $I_3 = \int_A x_3 dA$, $I_{33} = \int_A x_3^2 dA$, $I_{22} = \int_A x_2^2 dA$, $I_{23} = \int_A x_2 x_3 dA$, and $I_{rr} = \int_A \left(x_2^2 + x_3^2\right) dA$.
The matrix form of the above equations is

$$\boldsymbol{\sigma} = \mathbf{D}\mathbf{E} \tag{13}$$

where

$$\boldsymbol{\sigma} = \begin{Bmatrix} \sigma_1 \\ \sigma_2 \\ \sigma_3 \\ \sigma_4 \\ \sigma_5 \\ \sigma_6 \end{Bmatrix} = \begin{Bmatrix} N_{11} \\ M_{22} \\ M_{33} \\ T \\ Q_{12} \\ Q_{13} \end{Bmatrix} = \text{element generalized stresses} \tag{14}$$

$$\mathbf{E} = \mathbf{E}^L + \mathbf{E}^N = \begin{Bmatrix} E_1 \\ E_2 \\ E_3 \\ E_4 \\ E_5 \\ E_6 \end{Bmatrix} = \text{element generalized strains} \tag{15}$$

$$\mathbf{D} = \begin{bmatrix} EA & EI_2 & EI_3 & 0 & 0 & 0 \\ EI_2 & EI_{22} & EI_{23} & 0 & 0 & 0 \\ EI_3 & EI_{23} & EI_{33} & 0 & 0 & 0 \\ 0 & 0 & 0 & \mu I_{rr} & -\mu I_3 & \mu I_2 \\ 0 & 0 & 0 & -\mu I_3 & \mu k\mathrm{A} & 0 \\ 0 & 0 & 0 & \mu I_2 & 0 & \mu k\mathrm{A} \end{bmatrix} \tag{16}$$

where k is the shear coefficient related to the cross section, e.g., k is taken to be $2/3$ for the rectangular cross sections and k is taken to be 1.0 for the asymmetric cross sections in this paper.

$$\mathbf{E}^L = \begin{bmatrix} u_{10,1} & -u_{20,11} + \gamma_{2,1} & -u_{30,11} + \gamma_{3,1} & \theta_{1,1} & \gamma_2 & \gamma_3 \end{bmatrix}^T \tag{17}$$

$$\mathbf{E}^N = \begin{bmatrix} \frac{1}{2}\left(u_{20,1}^2 + u_{30,1}^2\right) & 0 & 0 & 0 & 0 & 0 \end{bmatrix}^T \tag{18}$$

3 Updated Lagrangian formulation in the co-rotational reference frame $\mathbf{e}_i$

3.1 The use of the Reissner variational principle in the co-rotational updated Lagrangian reference frame

If τ^0_{ij} are the initial Cauchy stresses in the updated Lagrangian co-rotational frame $\mathbf{e}_i$ of Fig.1, S^1_{ij} are the additional (incremental) second Piola-Kirchhoff stresses in the same updated Lagrangian co-rotational frame with axes $\mathbf{e}_i$, $S_{ij} = S^1_{ij} + \tau^0_{ij}$ are the total stresses, and u_i are the incremental displacements in the co-rotational updated-Lagrangian reference frame, the functional of the Reissner variational principle (Reissner 1953) [see also Atluri and Reissner 1989] for the incremental S^1_{ij} and u_i in the co-rotational updated Lagrangian reference frame is given by [Atluri 1979, 1980]

$$\Pi_R = \int_V \left\{ -B\left(S^1_{ij}\right) + \frac{1}{2}\tau^0_{ij} u_{k,\,i} u_{k,\,j} + \frac{1}{2} S_{ij}\left(u_{i,\,j} + u_{j,\,i}\right) - \rho b_i u_i \right\} dV - \int_{S_\sigma} \bar{T}_i u_i dS \tag{19}$$

where V is the volume in the current co-rotational reference state, S_σ is the surface where tractions are prescribed, $b_i = b^0_i + b^1_i$ are the body forces per unit volume in the current reference state, and $\bar{T}_i = \bar{T}^0_i + \bar{T}^1_i$ are the given boundary tractions.

The conditions of stationarity of Π_R, with respect to variations δS^1_{ij} and δu_i lead to the following incremental equations in the co-rotational updated- Lagrangian reference frame.

$$\frac{\partial B}{\partial S^1_{ij}} = \frac{1}{2}\left[u_{i,j} + u_{j,i}\right] \tag{20}$$

$$\left[S^1_{ij} + \tau^0_{ik} u_{j,k}\right]_{,\,j} + \rho b^1_i = -\left(\tau^0_{ij}\right)_{,\,j} - \rho b^0_i \tag{21}$$

$$n_j \left[S^1_{ij} + \tau^0_{ik} u_{j,k}\right]^{-} \bar{T}^1_i = -n_j \tau^0_{ij} + \bar{T}^0_i \text{ at } S_\sigma \tag{22}$$

In Eq.(19), the displacement boundary conditions,

$$u_i = \bar{u}_i \text{ at } S_u \tag{23}$$

are assumed to be satisfied a priori, at the external boundary, S_u. Eq.(21) leads to equilibrium correction iterations.

If the variational principle embodied in Eq.(19) is applied to a group of finite elements, $V_m, m = 1,2,\cdots,N$, which comprise the volume V, ie, $V = \sum V_m$, then

$$\Pi_R = \sum_m \left(\int_{V_m} \left\{ -B\left(S_{ij}^1\right) + \frac{1}{2}\tau_{ij}^0 u_{k,j} u_{k,j} + \frac{1}{2} S_{ij}\left(u_{i,j} + u_{j,i}\right) - \rho b_i u_i \right\} dV - \int_{S_{\sigma m}} \overline{T}_i u_i dS \right) \tag{24}$$

Let ∂V_m be the boundary of V_m, and ρ_m be the part of ∂V_m which is shared by the element with its neighbouring elements. If the trial function u_i and the test function ∂u_i in each V_m are such that the inter-element continuity condition,

$$u_i^+ = u_i^- \text{ at } \rho_m \tag{25}$$

(where + and – refer to either side of the boundary ρ_m) is satisfied a priori, then it can be shown (Atluri 1975,1984; Atluri and Murakawa 1977; Atluri, Gallagher and Zienkiewicz 1983) that the conditions of stationarity of Π_R in Eq.(24) lead to:

$$\frac{\partial B}{\partial S_{ij}^1} = \frac{1}{2}\left[u_{i,j} + u_{j,i}\right] \text{ in } V_m \tag{26}$$

$$\left[S_{ij}^1 + \tau_{ik}^0 u_{j,k}\right]_{,j} + \rho b_i^1 = -\tau_{ij,\,j}^0 - \rho b_i^0 \text{ in } V_m \tag{27}$$

$$\left[n_i\left(S_{ij}^1 + \tau_{ik}^0 u_{j,k}\right)\right]^+ + \left[n_i\left(S_{ij}^1 + \tau_{ik}^0 u_{j,k}\right)\right]^- = -\left[n_i \tau_{ij}^0\right]^+ - \left[n_i \tau_{ij}^0\right]^- \text{ at } \rho_m \tag{28}$$

$$n_j\left[S_{ij}^1 + \tau_{ik}^0 u_{j,k}\right]^- \bar{T}_i^1 = -n_j \tau_{ij}^0 + \bar{T}_i^0 \text{ at } S_{\sigma \mathrm{m}} \tag{29}$$

Eq.(28) is the condition of traction reciprocity at the inter-element boundary, ρ_m. Eqs. (27) and (28) lead to corrective iterations for equilibrium within each element, and traction reciprocity at the inter-element boundaries, respectively.

Carrying out the integration over the cross sectional area of each rod, and using Eqs.(4) and (12), Eq.(24) can be easily shown to reduce to:

$$\Pi_R = \sum_{elem} \left\{ \int_l \left(-\frac{1}{2}\boldsymbol{\sigma}^T \mathbf{D}^{-1} \boldsymbol{\sigma} \right) dl + \int_l N_{11}^0 \frac{1}{2}\left(u_{20,1}^2 + u_{30,1}^2\right) dl \right.$$
$$\left. + \int_l \left[\vec{N}_{11}\varepsilon_{11}^{0\mathrm{L}} + \vec{M}_{22}\left(\chi_{22} + \gamma_{2,1}\right) + \vec{M}_{33}\left(\chi_{33} + \gamma_{3,1}\right) + \vec{T}\theta_{11} + \vec{Q}_{12}\gamma_2 + \vec{Q}_{13}\gamma_3 \right] dl \right.$$
$$\left. - \bar{\mathbf{Q}}\mathbf{q} \right\} \tag{30}$$

where $\mathbf{D}$ is given in Eq.(16), $\mathbf{C}=\mathbf{D}^{-1}$, l is the length of the rod element, $\boldsymbol{\sigma}$ is given in Eq.(14), $\sigma_{ij}^{0}=\begin{bmatrix}N_{11}^{0} & M_{22}^{0} & M_{33}^{0} & T^{0} & Q_{12}^{0} & Q_{13}^{0}\end{bmatrix}^{T}$ is the initial element-generalized-stress in the corotational reference coordinates $\mathbf{e}_i$, and $\vec{\boldsymbol{\sigma}}=\boldsymbol{\sigma}^{0}+\boldsymbol{\sigma}=\begin{bmatrix}\vec{N}_{11} & \vec{M}_{22} & \vec{M}_{33} & \vec{T} & \vec{Q}_{12} & \vec{Q}_{13}\end{bmatrix}^{T}$ is the total element generalized stresses in the corotational reference coordinates $\mathbf{e}_i$. $\bar{\mathbf{Q}}$ is the nodal external generalized force vector (consisting of force as well as moments) in the global Cartesian reference frame, and $\mathbf{q}$ is the incremental nodal generalized displacement vector (consisting of displacements as well as rotations) in the global Cartesian reference frame. It should be noted that while Π_R in Eq.(30) represents a sum over the elements, the relevant integrals are evaluated over each element in it's own co-rotational updated Lagrangian reference frame.

By integrating by parts, the third item of the right side of Eq.(30) can be written as

$$\begin{aligned}
&\int_l \vec{N}_{11}\varepsilon_{11}^{0\mathrm{L}}dl=\int_l \vec{N}_{11}u_{10,1}dl\ =-\int_l \vec{N}_{11,1}u_{10}dl+\vec{N}_{11}u_{10}\Big|_0^l\\
&\int_l \vec{M}_{22}\left(\chi_{22}+\gamma_{2,1}\right)dl=-\int_l \vec{M}_{22}u_{20,11}dl+\int_l \vec{M}_{22}\gamma_{2,1}dl\\
&=-\int_l \vec{M}_{22,11}u_{20}dl+\vec{M}_{22,1}u_{20}\Big|_0^l-\vec{M}_{22}u_{20,1}\Big|_0^l-\int_l \vec{M}_{22,1}\gamma_2 dl+\vec{M}_{22}\gamma_2\Big|_0^l\\
&\int_l \vec{M}_{33}\left(\chi_{33}+\gamma_{3,1}\right)dl=-\int_l \vec{M}_{33}u_{30,11}dl+\int_l \vec{M}_{33}\gamma_{3,1}dl\\
&=-\int_l \vec{M}_{33,11}u_{30}dl+\vec{M}_{33,1}u_{30}\Big|_0^l-\vec{M}_{33}u_{30,1}\Big|_0^l-\int_l \vec{M}_{33,1}\gamma_3 dl+\vec{M}_{33}\gamma_3\Big|_0^l\\
&\int_l \vec{T}\theta_{1,1}dl=\int_l \vec{T}\theta_{1,1}dl\ =-\int_l \vec{T}_{,1}\theta_1 dl+\vec{T}\theta_1\Big|_0^l
\end{aligned}\tag{31}$$

The condition of stationarity of Π_R in Eq.(30) leads to:

$$\begin{aligned}
&\mathrm{D}^{-1}\sigma=E=\begin{bmatrix}u_{10,1} & -u_{20,11}+\gamma_{2,1} & -u_{30,11}+\gamma_{3,1} & \theta_{1,1} & \gamma_2 & \gamma_3\end{bmatrix}^{T}\\
&\vec{N}_{11,1}=0 \text{ in each element}\\
&\vec{T}_{,1}=0 \text{ in each element}\\
&\vec{M}_{22,11}+\left(N_{11}^{0}u_{20,1}\right)_{,1}=0 \text{ in each element}\\
&\vec{M}_{33,11}+\left(N_{11}^{0}u_{30,1}\right)_{,1}=0 \text{ in each element}\\
&-\vec{M}_{22,1}+\vec{Q}_{12}=0 \text{ in each element}\\
&-\vec{M}_{33,1}+\vec{Q}_{13}=0 \text{ in each element}
\end{aligned}\tag{32}$$

and the nodal equilibrium equations, which arise out of the term:

$$\sum_{elem}\Big\{\vec{N}_{11}\delta u_{10}\,\big|_0^l+\vec{M}_{22,1}\delta u_{20}\,\big|_0^l-\vec{M}_{22}\delta u_{20,1}\,\big|_0^l+\vec{M}_{22}\delta\gamma_2\Big|_0^l \\ +\vec{M}_{33,1}\delta u_{30}\,\big|_0^l-\vec{M}_{33}\delta u_{30,1}\,\big|_0^l \\ +\vec{M}_{33}\delta\gamma_3\Big|_0^l+\vec{T}\delta\,\theta_1|_0^l+\left(N_{11}^0u_{20,1}\right)\delta\,u_{20}|_0^l+\left(N_{11}^0u_{30,1}\right)\delta\,u_{30}|_0^l-\bar{\mathbf{Q}}\delta\mathbf{q}\Big\}=0 \tag{33}$$

3.2 Trial functions of the stresses and displacements in each element

We assume the trial functions for $N_{11},M_{22},M_{33},T,Q_{12}$ and Q_{13} in each element, as

$$\begin{aligned} N_{11}&=n\\ M_{22}&=-m_3=-\phi_1{}^1m_3-\phi_2{}^2m_3\\ M_{33}&=m_2=\phi_1{}^1m_2+\phi_2{}^2m_2\\ T&=m_1\\ Q_{12}&=\phi_1{}^1q_2+\phi_2{}^2q_2\\ Q_{13}&=\phi_1{}^1q_3+\phi_2{}^2q_3 \end{aligned} \tag{34}$$

where

$$\begin{aligned} &\phi_1=1-\xi\\ &\phi_2=\xi \end{aligned}\qquad\left(\xi=\frac{x_1}{l}\right) \tag{35}$$

The matrix form of the above equation is

$$\boldsymbol{\sigma}=\mathbf{P}\beta \tag{36}$$

where

$$\mathbf{P}=\begin{bmatrix} 1 & 0 & 0 & 0 & 0 & 0 & 0 & 0 & 0 & 0\\ 0 & -\phi_1 & -\phi_2 & 0 & 0 & 0 & 0 & 0 & 0 & 0\\ 0 & 0 & 0 & \phi_1 & \phi_2 & 0 & 0 & 0 & 0 & 0\\ 0 & 0 & 0 & 0 & 0 & 1 & 0 & 0 & 0 & 0\\ 0 & 0 & 0 & 0 & 0 & 0 & \phi_1 & \phi_2 & 0 & 0\\ 0 & 0 & 0 & 0 & 0 & 0 & 0 & 0 & \phi_1 & \phi_2 \end{bmatrix} \tag{37}$$

$$\boldsymbol{\beta}=\begin{bmatrix} n & {}^1m_3 & {}^2m_3 & {}^1m_2 & {}^2m_2 & m_1 & {}^1q_2 & {}^2q_2 & {}^1q_3 & {}^2q_3 \end{bmatrix}^T \tag{38}$$

In a same way, the initial stress $\boldsymbol{\sigma}^0$ can be expressed as

$$\boldsymbol{\sigma}^0 = \mathbf{P}\beta^0 \tag{39}$$

where

$$\boldsymbol{\beta}^0 = \begin{bmatrix} n^0 & {}^1m_3^0 & {}^2m_3^0 & {}^1m_2^0 & {}^2m_2^0 & m_1^0 & {}^1q_2^0 & {}^2q_2^0 & {}^1q_3^0 & {}^2q_3^0 \end{bmatrix}^T \tag{40}$$

The incremental internal nodal force vector $\boldsymbol{\beta}_n$ of node 1 and node 2 of a rod is denoted as

$$\boldsymbol{\beta}_n = \begin{bmatrix} {}^1N & {}^1q_2 & {}^1q_3 & {}^1m_1 & {}^1m_2 & {}^1m_3 & {}^2N & {}^2q_2 & {}^2q_3 & {}^2m_1 & {}^2m_2 & {}^2m_3 \end{bmatrix}^T \tag{41}$$

In the functional in Eq.(30), only γ_2, γ_3, and the squares of $u_{20,1}$ and $u_{30,1}$ occur within each element. Thus, $\vec{\theta}_2 = -u_{30,1}$ and $\vec{\theta}_3 = u_{20,1}$ are assumed directly to be linear within each element, in terms of their respective nodal values. This will be enormously simple and advantageous in the case of plate and shell elements. This is in contrast to the primal approach (Zhu, Cai, Paik and Atluri 2010) wherein u_{20} and u_{30} were required to be C^1 continuous over each element, and thus were assumed to be Herimitian polynomials over each element. In this paper, however, we assume:

$$\mathbf{u}_\theta = \begin{Bmatrix} \vec{\theta}_2 \\ \vec{\theta}_3 \end{Bmatrix} = \mathbf{N}_\theta \mathbf{a}_\theta = \begin{bmatrix} \phi_1 & 0 & \phi_2 & 0 \\ 0 & \phi_1 & 0 & \phi_2 \end{bmatrix} \begin{Bmatrix} {}^1\vec{\theta}_2 \\ {}^1\vec{\theta}_3 \\ {}^2\vec{\theta}_2 \\ {}^2\vec{\theta}_3 \end{Bmatrix} \tag{42}$$

Assuming that '**a**' represents the vector of generalized displacements of the nodes of the rod element in the updated Lagrangian co-rotational frame $\mathbf{e}_i$ of Fig.1, the displacement vectors of node i are:

$$\begin{aligned} {}^i\mathbf{a} &= \begin{bmatrix} {}^iu_1 & {}^iu_2 & {}^iu_3 & {}^iu_4 & {}^iu_5 & {}^iu_6 & {}^iu_7 & {}^iu_8 \end{bmatrix}^T \\ &= \begin{bmatrix} {}^iu_{10} & {}^iu_{20} & {}^iu_{30} & {}^i\theta_1 & {}^i\vec{\theta}_2 & {}^i\vec{\theta}_3 & {}^i\gamma_3 & {}^i\gamma_2 \end{bmatrix}^T \quad [i = 1,2] \end{aligned} \tag{43}$$

where ${}^i\vec{\theta}_2 = -{}^iu_{30,1}$ and ${}^i\vec{\theta}_3 = {}^iu_{20,1}$.

The relation between $\mathbf{a}_\theta$ and $\mathbf{a}$ can be expressed as

$$\mathbf{a}_\theta = \mathbf{T}_\theta \mathbf{a} \tag{44}$$

where

$$\mathbf{T}_\theta = \begin{bmatrix} 0 & 0 & 0 & 0 & 1 & 0 & 0 & 0 & 0 & 0 & 0 & 0 & 0 & 0 & 0 & 0 \\ 0 & 0 & 0 & 0 & 0 & 1 & 0 & 0 & 0 & 0 & 0 & 0 & 0 & 0 & 0 & 0 \\ 0 & 0 & 0 & 0 & 0 & 0 & 0 & 0 & 0 & 0 & 0 & 0 & 1 & 0 & 0 & 0 \\ 0 & 0 & 0 & 0 & 0 & 0 & 0 & 0 & 0 & 0 & 0 & 0 & 0 & 1 & 0 & 0 \end{bmatrix} \tag{45}$$

$\gamma_2$and γ_3 can also be assumed as

$$\mathbf{u}_\gamma = \begin{Bmatrix} \gamma_2 \\ \gamma_3 \end{Bmatrix} = \mathbf{N}_\gamma \mathbf{a}_\gamma = \begin{bmatrix} \phi_1 & 0 & \phi_2 & 0 \\ 0 & \phi_1 & 0 & \phi_2 \end{bmatrix} \begin{Bmatrix} {}^1\gamma_2 \\ {}^1\gamma_3 \\ {}^2\gamma_2 \\ {}^2\gamma_3 \end{Bmatrix} \tag{46}$$

3.3 Explicit expressions of the tangent stiffness matrix for each element

Because of the assumption of the trial functions of the stresses in Eq.(34), the following items in Eq.(31) become

$$\begin{aligned} \int_l \vec{N}_{11,1} u_{10} dl &= 0 \\ \int_l \vec{M}_{22,11} u_{20} dl &= 0 \\ \int_l \vec{M}_{33,11} u_{30} dl &= 0 \\ \int_l \vec{T}_{,1} \theta_1 dl &= 0 \end{aligned} \tag{47}$$

Eq.(30) can be rewritten as

$$\Pi_R = -\Pi_{R1} + \Pi_{R2} + \Pi_{R3} - \Pi_{R4} \tag{48}$$

where

$$\Pi_{R1} = \sum_{elem} \int_l \left(\frac{1}{2} \boldsymbol{\sigma}^T \mathbf{D}^{-1} \boldsymbol{\sigma} \right) dl = \sum_{elem} \int_l \left(\frac{1}{2} \boldsymbol{\beta}^T \mathbf{P}^T \mathbf{C} \mathbf{P} \boldsymbol{\beta} \right) dl \tag{49}$$

$$\begin{aligned}\Pi_{R2} &= \sum_{elem}\left\{{}^2N^2u_{10} - {}^1N^1u_{10} + \frac{1}{l}\left({}^1m_3 - {}^2m_3\right)\left({}^2u_{20} - {}^1u_{20}\right) + {}^2m_3{}^2\vec{\theta}_3 - {}^1m_3{}^1\vec{\theta}_3\right.\\ &+ \frac{1}{l}\left({}^2m_2 - {}^1m_2\right)\left({}^2u_{30} - {}^1u_{30}\right) + {}^2m_2{}^2\vec{\theta}_2 - {}^1m_2{}^1\vec{\theta}_2 + {}^2m_1{}^2\theta_1 - {}^1m_1{}^1\theta_1\\ &- {}^2m_3{}^2\gamma_2 + {}^1m_3{}^1\gamma_2 + {}^2m_2{}^2\gamma_3 - {}^1m_2{}^1\gamma_3 + \frac{l}{6}\left(2{}^1q_2{}^1\gamma_2 + {}^1q_2{}^2\gamma_2\right.\\ &\left.\left.+ {}^2q_2{}^1\gamma_2 + 2{}^2q_2{}^2\gamma_2 + 2{}^1q_3{}^1\gamma_3 + {}^1q_3{}^2\gamma_3 + {}^2q_3{}^1\gamma_3 + {}^2q_3{}^2\gamma_3\right)\right\}\\ &= \sum_{elem}\left\{(\boldsymbol{\beta})^T\,\mathbf{R}_\sigma\mathbf{a}\right\}\end{aligned} \tag{50}$$

where

$$\mathbf{R}_\sigma = \begin{bmatrix} -1 & 0 & 0 & 0 & 0 & 0 & 0 & 0 & 1 & 0 & 0 & 0 & 0 & 0 & 0 \\ 0 & -\frac{1}{l} & 0 & 0 & 0 & -1 & 0 & \frac{1}{2} & 0 & \frac{1}{l} & 0 & 0 & 0 & 0 & -\frac{1}{2} \\ 0 & \frac{1}{l} & 0 & 0 & 0 & 0 & 0 & \frac{1}{2} & 0 & -\frac{1}{l} & 0 & 0 & 0 & 1 & 0 & -\frac{1}{2} \\ 0 & 0 & \frac{1}{l} & 0 & -1 & 0 & -\frac{1}{2} & 0 & 0 & 0 & -\frac{1}{l} & 0 & 0 & 0 & \frac{1}{2} & 0 \\ 0 & 0 & -\frac{1}{l} & 0 & 0 & 0 & -\frac{1}{2} & 0 & 0 & 0 & \frac{1}{l} & 0 & 0 & 0 & \frac{1}{2} & 0 \\ 0 & 0 & 0 & -1 & 0 & 0 & 0 & 0 & 0 & 0 & 0 & 1 & 0 & 0 & 0 & 0 \\ 0 & 0 & 0 & 0 & 0 & 0 & 0 & \frac{l}{3} & 0 & 0 & 0 & 0 & 0 & 0 & 0 & \frac{l}{6} \\ 0 & 0 & 0 & 0 & 0 & 0 & 0 & \frac{l}{6} & 0 & 0 & 0 & 0 & 0 & 0 & 0 & \frac{l}{3} \\ 0 & 0 & 0 & 0 & 0 & 0 & \frac{l}{3} & 0 & 0 & 0 & 0 & 0 & 0 & 0 & \frac{l}{6} & 0 \\ 0 & 0 & 0 & 0 & 0 & 0 & \frac{l}{6} & 0 & 0 & 0 & 0 & 0 & 0 & 0 & \frac{l}{3} & 0 \end{bmatrix} \tag{51}$$

In Π_{R2}, only the element nodal values of the transverse displacements, derivatives of the transverse displacements, and transverse shear strains appear. Thus, for evaluating Π_{R2}, one need not assume these trial functions over the element.

$$\begin{aligned}\Pi_{R3} &= \sum_{elem}\int_l N_{11}^0\left[\frac{1}{2}\left(u_{20,1}\right)^2 + \frac{1}{2}\left(u_{30,1}\right)^2\right]dl = \sum_{elem}\int_l \sigma_1^0\left[\frac{1}{2}\left(\vec{\theta}_2\right)^2 + \frac{1}{2}\left(\vec{\theta}_3\right)^2\right]dl\\ &= \sum_{elem}\int_l \frac{\sigma_1^0}{2}\mathbf{u}_\theta^T\mathbf{u}_\theta dl = \sum_{elem}\int_l \frac{\sigma_1^0}{2}\mathbf{a}^T\mathbf{T}_\theta^T\mathbf{N}_\theta^T\mathbf{N}_\theta\mathbf{T}_\theta\mathbf{a}dl\end{aligned} \tag{52}$$

in Π_{R3}, only the squares of $u_{20,1}$ and $u_{30,1}$ appear over each element. Thus, $u_{20,1}$ and $u_{30,1}$ are simply assumed to be C^0 continuous over each element.

Letting $\mathbf{A}_{nn} = \mathbf{T}_\theta^T \mathbf{N}_\theta^T \mathbf{N}_\theta \mathbf{T}_\theta$, Π_{R3} can be rewritten as

$$\Pi_{R3} = \sum_{elem} \int_l \frac{\sigma_1^0}{2} \mathbf{a}^T \mathbf{A}_{nn} \mathbf{a} dl \tag{53}$$

and

$$\Pi_{R4} = \sum_{elem} \left(\mathbf{a}^T \mathbf{F} - \mathbf{a}^T \mathbf{R}_\sigma^T \boldsymbol{\beta}^0 \right) \tag{54}$$

Thus, in summary, in the present development of a (16x16) *symmetric* tangent stiffness matrix for a thick/thin beam element which undergoes large rotations over each element we need only assume:

1. C^0 continuous functions over the element for $u_{20,1}$ and $u_{30,1}$
2. C^0 continuous functions over each element for M_{22} and M_{33}
3. C^0 continuous functions over each element for Q_{12} and Q_{13}, and
4. a constant over each element for T.

Thus, the present development based on the Reissner's varitional principle is much simpler than that based on the primal method in Zhu, Cai, Paik and Atluri (2010). *This simplicity of the present method will be far more pronounced when plate and shell elements developed.*

By invoking $\delta\, \Pi_R = 0$, we can obtain

$$\begin{aligned} \delta \Pi_R = & \sum_{elem} \delta \boldsymbol{\beta}^T \left\{ - \int_l \mathbf{P}^T \mathbf{C} \mathbf{P} \beta dl + \mathbf{R}_\sigma \mathbf{a} \right\} + \\ & \sum_{elem} \delta \mathbf{a}^T \left\{ \mathbf{R}_\sigma^T \boldsymbol{\beta} + \sigma_1^0 \int_l \mathbf{A}_{nn} \mathbf{a} dl + \mathbf{R}_\sigma^T \boldsymbol{\beta}^0 - \mathbf{F} \right\} \end{aligned} \tag{55}$$

Let

$$\mathbf{H} = \int_l \mathbf{P}^T \mathbf{C} \mathbf{P} dl, \quad \mathbf{G} = \mathbf{R}_\sigma, \quad \mathbf{K}_N = \sigma_1^0 \int_l \mathbf{A}_{nn} dl, \quad \mathbf{F}^0 = \mathbf{G}^T \boldsymbol{\beta}^0 \tag{56}$$

then

$$\delta \Pi_R = \sum_{elem} \delta \boldsymbol{\beta}^T \left\{ -\mathbf{H} \beta + \mathbf{G} \mathbf{a} \right\} - \sum_{elem} \delta \mathbf{a}^T \left\{ \mathbf{G}^T \boldsymbol{\beta} + \mathbf{K}_N \mathbf{a} - \mathbf{F} + \mathbf{F}^0 \right\} = 0 \tag{57}$$

Since $\delta\,\boldsymbol{\beta}^T$ in Eq.(57) are independent and arbitrary in each element, one obtains

$$\boldsymbol{\beta} = \mathbf{H}^{-1}\mathbf{G}\mathbf{a} \tag{58}$$

and

$$\sum_{elem} \delta\mathbf{a}^T \left\{ \left(\mathbf{K}_L + \mathbf{K}_N\right)\mathbf{a} - \mathbf{F} + \mathbf{F}^0 \right\} = 0 \tag{59}$$

where

$$\mathbf{K}_L = \mathbf{G}^T\mathbf{H}^{-1}\mathbf{G} \tag{60}$$

$$\mathbf{K}_N = \sigma_1^0 \int_l \mathbf{A}_{nn} dl \tag{61}$$

The components of the element tangent stiffness matrix, $\mathbf{K}_L$ and $\mathbf{K}_N$, respectively, can be derived explicitly, after some simple algebra, as follows.

$$\mathbf{K}_N = \frac{l\sigma_1^0}{6} \begin{bmatrix} 0 & 0 & 0 & 0 & 0 & 0 & 0 & 0 & 0 & 0 & 0 & 0 & 0 & 0 & 0 & 0 \\ & 0 & 0 & 0 & 0 & 0 & 0 & 0 & 0 & 0 & 0 & 0 & 0 & 0 & 0 & 0 \\ & & 0 & 0 & 0 & 0 & 0 & 0 & 0 & 0 & 0 & 0 & 0 & 0 & 0 & 0 \\ & & & 0 & 0 & 0 & 0 & 0 & 0 & 0 & 0 & 0 & 0 & 0 & 0 & 0 \\ & & & & 2 & 0 & 0 & 0 & 0 & 0 & 0 & 0 & 1 & 0 & 0 & 0 \\ & & & & & 2 & 0 & 0 & 0 & 0 & 0 & 0 & 0 & 1 & 0 & 0 \\ & & & & & & 0 & 0 & 0 & 0 & 0 & 0 & 0 & 0 & 0 & 0 \\ & & & & & & & 0 & 0 & 0 & 0 & 0 & 0 & 0 & 0 & 0 \\ & & & & & & & & 0 & 0 & 0 & 0 & 0 & 0 & 0 & 0 \\ & & & & & & & & & 0 & 0 & 0 & 0 & 0 & 0 & 0 \\ & & & & sym. & & & & & & 0 & 0 & 0 & 0 & 0 & 0 \\ & & & & & & & & & & & 0 & 0 & 0 & 0 & 0 \\ & & & & & & & & & & & & 2 & 0 & 0 & 0 \\ & & & & & & & & & & & & & 2 & 0 & 0 \\ & & & & & & & & & & & & & & 0 & 0 \\ & & & & & & & & & & & & & & & 0 \end{bmatrix} \tag{62}$$

$$\mathbf{K}_L = \frac{E}{lA} \begin{bmatrix} \mathbf{K}_{L1} & \mathbf{K}_{L12} \\ \mathbf{K}_{L12}^T & \mathbf{K}_{L2} \end{bmatrix} \tag{63}$$

where

$$\mathbf{K}_{L1} = \begin{bmatrix} A^2 & 0 & 0 & 0 & AI_3 & -AI_2 & AI_3 & AI_2 \\ & a_1 & a_2 & 0 & -a_3 & a_4 & 0 & 0 \\ & & a_5 & 0 & -a_6 & a_3 & 0 & 0 \\ & & & a_7 & 0 & 0 & -a_{10}I_2 & a_{10}I_3 \\ & & & & a_8 & a_9 & AI_{33} & AI_{23} \\ & & sym. & & & a_{13} & -AI_{23} & -AI_{22} \\ & & & & & & a_{15} & a_{17} \\ & & & & & & & a_{19} \end{bmatrix} \tag{64}$$

$$\mathbf{K}_{L2} = \begin{bmatrix} A^2 & 0 & 0 & 0 & AI_3 & -AI_2 & AI_3 & AI_2 \\ & a_1 & a_2 & 0 & a_3 & -a_4 & 0 & 0 \\ & & a_5 & 0 & a_6 & -a_3 & 0 & 0 \\ & & & a_7 & 0 & 0 & a_{10}I_2 & -a_{10}I_3 \\ & & & & a_8 & a_9 & AI_{33} & AI_{23} \\ & & sym. & & & a_{13} & -AI_{23} & -AI_{22} \\ & & & & & & a_{15} & a_{17} \\ & & & & & & & a_{19} \end{bmatrix} \tag{65}$$

$$\mathbf{K}_{L12} = \begin{bmatrix} -A^2 & 0 & 0 & 0 & -AI_3 & AI_2 & -AI_3 & -AI_2 \\ 0 & -a_1 & -a_2 & 0 & -a_3 & a_4 & 0 & 0 \\ 0 & -a_2 & -a_5 & 0 & -a_6 & a_3 & 0 & 0 \\ 0 & 0 & 0 & -a_7 & 0 & 0 & -a_{10}I_2 & a_{10}I_3 \\ -AI_3 & a_3 & a_6 & 0 & a_{11} & a_{12} & -AI_{33} & -AI_{23} \\ AI_2 & -a_4 & -a_3 & 0 & a_{12} & a_{14} & AI_{23} & AI_{22} \\ -AI_3 & 0 & 0 & a_{10}I_2 & -AI_{33} & AI_{23} & -a_{16} & -a_{17} \\ -AI_2 & 0 & 0 & -a_{10}I_3 & -AI_{23} & AI_{22} & -a_{17} & -a_{18} \end{bmatrix} \tag{66}$$

where $a_1 = 12\left(AI_{22} - I_2^2\right)/l^2$, $a_2 = 12\left(AI_{23} - I_2I_3\right)/l^2$, $a_3 = 6\left(AI_{23} - I_2I_3\right)/l$, $a_4 = 6\left(AI_{22} - I_2^2\right)/l$, $a_5 = 12\left(AI_{33} - I_3^2\right)/l^2$, $a_6 = 6\left(AI_{33} - I_3^2\right)/l$, $a_7 = A\mu I_{rr}/E$, $a_8 = 4AI_{33} - 3I_3^2$, $a_9 = -4AI_{23} + 3I_2I_3$, $a_{10} = 0.5A\mu l/E$, $a_{11} = 2AI_{33} - 3I_3^2$, $a_{12} = -2AI_{23} + 3I_2I_3$, $a_{13} = 4AI_{22} - 3I_2^2$, $a_{14} = 2AI_{22} - 3I_2^2$, $a_{15} = AI_{33} + \mu kA^2l^2/(3E) - A\mu I_2^2l^2/(12EI_{rr})$, $a_{16} = AI_{33} - \mu kA^2l^2/(6E) - A\mu I_2^2l^2/(12EI_{rr})$, $a_{17} = AI_{23} + \mu AI_2I_3l^2/(12EI_{rr})$, $a_{18} = AI_{22} - \mu kA^2l^2/(6E) - A\mu I_3^2l^2/(12EI_{rr})$, and $a_{19} = AI_{22} + \mu kA^2l^2/(3E) - A\mu I_3^2l^2/(12EI_{rr})$.

Thus, $\mathbf{K}_L$ is the usual linear symmetric (16×16) stiffness matrix of the beam in the co-rotational reference frame, with the geometric parameters I_2, I_3, I_{22}, I_{33}, I_{23}, I_{rr}, and the current length l.

The external equivalent nodal force in Eq.(59) can also be simplified to

$$\mathbf{F}^0 = \left[\begin{array}{cccccccc} -\sigma_1^0 & -\frac{\sigma_2^0-\sigma_3^0}{l} & \frac{\sigma_4^0-\sigma_5^0}{l} & -\sigma_6^0 & -\sigma_4^0 & -\sigma_2^0 & c_1 & c_2 \\ \sigma_1^0 & \frac{\sigma_2^0-\sigma_3^0}{l} & -\frac{\sigma_4^0-\sigma_5^0}{l} & \sigma_6^0 & \sigma_5^0 & \sigma_3^0 & c_3 & c_4 \end{array} \right]^T \tag{67}$$

where $c_1 = -\frac{\sigma_4^0+\sigma_5^0}{2} + \frac{l}{6}\left(2\sigma_9^0+\sigma_{10}^0\right)$, $c_2 = \frac{\sigma_2^0+\sigma_3^0}{2} + \frac{l}{6}\left(2\sigma_7^0+\sigma_8^0\right)$, $c_3 = \frac{\sigma_4^0+\sigma_5^0}{2} + \frac{l}{6}\left(\sigma_9^0+2\sigma_{10}^0\right)$ and $c_4 = -\frac{\sigma_2^0+\sigma_3^0}{2} + \frac{l}{6}\left(\sigma_7^0+2\sigma_8^0\right)$.

The items c_1, c_2, c_1, and c_4 of the external equivalent nodal force in Eq.(67) can also be simplified to $c_1 = 0$, $c_2 = 0$, $c_3 = 0$ and $c_4 = 0$. Numerical examples indicate that the simplification could dramatically accelerate the convergence rates of the large deformation analyses of the shear flexible beam element in some cases, however, it would not impair the accuracy of the results.

It is clear from the above procedures, that the present (16×16) symmetric tangent stiffness matrices of the beam in the co-rotational reference frame, based on the Reissner variational principle and simplified rod theory, are much simpler than those of Kondoh, Tanaka and Atluri (1986), Kondoh and Atluri (1987), and Shi and Atluri (1988). Moreover, the explicit expressions for the tangent stiffness matrix of each rod can be seen to be derived as text-book examples of nonlinear analyses.

4 Transformation between deformation dependent co-rotational local $[\mathbf{e}_i]$, and the global $[\bar{\mathbf{e}}_i]$ frames of reference

As shown in Fig.1, $\bar{x}_i\,(i=1,2,3)$ are the global coordinates with unit basis vectors $\bar{\mathbf{e}}_i$. $\tilde{x}_i$ and $\tilde{\mathbf{e}}_i$ are the local coordinates for the rod element at the undeformed element. The basis vector $\tilde{\mathbf{e}}_i$ are initially chosen such that (Shi and Atluri 1988)

$$\begin{aligned} \tilde{\mathbf{e}}_1 &= (\Delta\tilde{x}_1\bar{\mathbf{e}}_1 + \Delta\tilde{x}_2\bar{\mathbf{e}}_2 + \Delta\tilde{x}_3\bar{\mathbf{e}}_3)/L \\ \tilde{\mathbf{e}}_2 &= (\bar{\mathbf{e}}_3 \times \tilde{\mathbf{e}}_1)/|\bar{\mathbf{e}}_3 \times \tilde{\mathbf{e}}_1| \\ \tilde{\mathbf{e}}_3 &= \tilde{\mathbf{e}}_1 \times \tilde{\mathbf{e}}_2 \end{aligned} \tag{68}$$

where $\Delta\tilde{x}_i = \tilde{x}_i^2 - \tilde{x}_i^1$, $L = \left(\Delta\tilde{x}_1^2 + \Delta\tilde{x}_2^2 + \Delta\tilde{x}_3^2\right)^{\frac{1}{2}}$.

Then $\tilde{\mathbf{e}}_i$ and $\bar{\mathbf{e}}_i$ have the following relations:

$$\begin{Bmatrix} \tilde{\mathbf{e}}_1 \\ \tilde{\mathbf{e}}_2 \\ \tilde{\mathbf{e}}_3 \end{Bmatrix} = \begin{bmatrix} \Delta\tilde{x}_1/L & \Delta\tilde{x}_2/L & \Delta\tilde{x}_3/L \\ -\Delta\tilde{x}_2/S & \Delta\tilde{x}_1/S & 0 \\ -\Delta\tilde{x}_1\Delta\tilde{x}_3/(SL) & -\Delta\tilde{x}_2\Delta\tilde{x}_3/(SL) & s/L \end{bmatrix} \begin{Bmatrix} \bar{\mathbf{e}}_1 \\ \bar{\mathbf{e}}_2 \\ \bar{\mathbf{e}}_3 \end{Bmatrix} \tag{69}$$

where $S = \left(\Delta\tilde{x}_1^2 + \Delta\tilde{x}_2^2\right)^{\frac{1}{2}}$.

Thus we can define a transformation matrix $\tilde{\boldsymbol{\lambda}}_0$ between $\tilde{\mathbf{e}}_i$ and $\bar{\mathbf{e}}_i$ as

$$\tilde{\boldsymbol{\lambda}}_0 = \begin{bmatrix} \Delta\tilde{x}_1/L & \Delta\tilde{x}_2/L & \Delta\tilde{x}_3/L \\ -\Delta\tilde{x}_2/S & \Delta\tilde{x}_1/S & 0 \\ -\Delta\tilde{x}_1\Delta\tilde{x}_3/(SL) & -\Delta\tilde{x}_2\Delta\tilde{x}_3/(SL) & S/L \end{bmatrix} \tag{70}$$

When the element is parallel to the $\bar{x}_3$ axis, $S = \left[\Delta\tilde{x}_1^2 + \Delta\tilde{x}_2^2\right]^{\frac{1}{2}} = 0$ and Eq.(69) is not valid. In this case, the local coordinates is determined by

$$\tilde{\mathbf{e}}_1 = \bar{\mathbf{e}}_3, \tilde{\mathbf{e}}_2 = \bar{\mathbf{e}}_2, \tilde{\mathbf{e}}_3 = -\bar{\mathbf{e}}_1 \tag{71}$$

Let x_i and $\mathbf{e}_i$ be the co-rotational reference coordinates for the deformed rod element. In order to continuously define the local coordinates of the same rod element during the whole range of large deformation, the basis vectors $\mathbf{e}_i$ are chosen such that

$$\begin{aligned} \mathbf{e}_1 &= (\Delta x_1\bar{\mathbf{e}}_1 + \Delta x_2\bar{\mathbf{e}}_2 + \Delta x_3\bar{\mathbf{e}}_3)/l = a_1\bar{\mathbf{e}}_1 + a_2\bar{\mathbf{e}}_2 + a_3\bar{\mathbf{e}}_3 \\ \mathbf{e}_2 &= (\tilde{\mathbf{e}}_3 \times \mathbf{e}_1)/|\tilde{\mathbf{e}}_3 \times \mathbf{e}_1| \\ \mathbf{e}_3 &= \mathbf{e}_1 \times \mathbf{e}_2 \end{aligned} \tag{72}$$

where $\Delta x_i = x_i^2 - x_i^1$, $l = \left(\Delta x_1^2 + \Delta x_2^2 + \Delta x_3^2\right)^{\frac{1}{2}}$.
We denote $\tilde{\mathbf{e}}_3$ in Eq.(69) as

$$\tilde{\mathbf{e}}_3 = c_1\bar{\mathbf{e}}_1 + c_2\bar{\mathbf{e}}_2 + c_3\bar{\mathbf{e}}_3 \tag{73}$$

Then $\mathbf{e}_i$ and $\bar{\mathbf{e}}_i$ have the following relations:

$$\begin{Bmatrix} \mathbf{e}_1 \\ \mathbf{e}_2 \\ \mathbf{e}_3 \end{Bmatrix} = \begin{bmatrix} a_1 & a_2 & a_3 \\ b_1 & b_2 & b_3 \\ a_2b_3 - a_3b_2 & a_3b_1 - a_1b_3 & a_1b_2 - a_2b_1 \end{bmatrix} \begin{Bmatrix} \bar{\mathbf{e}}_1 \\ \bar{\mathbf{e}}_2 \\ \bar{\mathbf{e}}_3 \end{Bmatrix} = \boldsymbol{\lambda}_0\bar{\mathbf{e}}_i \tag{74}$$

where

$$\begin{aligned} b_1 &= (c_2a_3 - c_3a_2)/l_{31} \\ b_2 &= (c_3a_1 - c_1a_3)/l_{31} \\ b_3 &= (c_1a_2 - c_2a_1)/l_{31} \end{aligned} \tag{75}$$

$$l_{31} = \left[(c_2a_3 - c_3a_2)^2 + (c_3a_1 - c_1a_3)^2 + (c_1a_2 - c_2a_1)^2\right]^{\frac{1}{2}} \tag{76}$$

and

$$\boldsymbol{\lambda}_0 = \begin{bmatrix} a_1 & a_2 & a_3 \\ b_1 & b_2 & b_3 \\ a_2b_3 - a_3b_2 & a_3b_1 - a_1b_3 & a_1b_2 - a_2b_1 \end{bmatrix} \tag{77}$$

Thus, the transformation matrix $\boldsymbol{\lambda}$, between the 16 generalized coordinates in the co-rotational reference frame, and the corresponding 16 coordinates in the global Cartesian reference frame, is given by

$$\boldsymbol{\lambda} = \begin{bmatrix} {}^1\boldsymbol{\lambda} & \\ & {}^2\boldsymbol{\lambda} \end{bmatrix} \tag{78}$$

where

$${}^i\boldsymbol{\lambda} = \begin{bmatrix} \boldsymbol{\lambda}_0 & 0 & 0 & 0 \\ 0 & \boldsymbol{\lambda}_0 & 0 & 0 \\ 0 & 0 & b_2 & b_3 \\ 0 & 0 & a_3b_1 - a_1b_3 & a_1b_2 - a_2b_1 \end{bmatrix} \tag{79}$$

Letting x_i and $\mathbf{e}_i$ be the reference coordinates, and repeating the above steps [Eq.(72) – Eq.(79)], the transformation matrix of each incremental step can be obtained in a same way.

If a single straight beam is discretized into finite elements, one may enforce the nodal continuity of ($\vec{\theta}_2$ and γ_2) as well as ($\vec{\theta}_3$ and γ_3) separately, thus leading to the nodal continuity of the total rotations θ_2 and θ_3 respectively. However, when two or more beams are connected arbitrarily at a node, as in a space-frame, geometric compatibility requires the nodal connectivity of only the global Cartesian components of θ_2 and θ_3 of the beams joined at the node. However, for algebraic simplicity, and with some sacrifice of theoretical exactness, only the nodal connectivity of the global Cartesian components of ($\vec{\theta}_2$ and $\vec{\theta}_3$) as well as of (γ_2 and γ_3) are enforced separately, in this paper.

Then the element matrices are transformed to the global coordinate system using

$$\bar{\mathbf{a}} = \boldsymbol{\lambda}^T \mathbf{a} \tag{80}$$

$$\bar{\mathbf{K}} = \boldsymbol{\lambda}^T \mathbf{K} \boldsymbol{\lambda} \tag{81}$$

$$\bar{\mathbf{F}} = \boldsymbol{\lambda}^T \mathbf{F} \tag{82}$$

where $\bar{\mathbf{a}}, \bar{\mathbf{K}}, \bar{\mathbf{F}}$ are respectively the generalized nodal displacements, element tangent stiffness matrix and generalized nodal forces, in the global coordinates system.

After assembling the element stiffness matrices and nodal force vectors, into their global counterparts, we obtain the discretized equations of the space frames as

$$\hat{\mathbf{K}}\hat{\mathbf{a}} = \hat{\mathbf{F}} - \hat{\mathbf{F}}^0 \tag{83}$$

The Newton-Raphson method, modified Newton-Rapson method or the artificial time integration method (Liu 2007a, 2007b; Liu and Atluri 2008) can be employed to solve Eq.(83). In this implementation, the Newton-Raphson algorithm is used.

5 Numerical examples

5.1 A cantilever beam with a symmetric cross section

A large deflection and moderate rotation analysis of a cantilever beam subject to a transverse load at the tip, as shown in Fig. 3, is considered. The cross section of the beam is a square. The Poisson's ration is $\nu = 0.25$. The transverse load at the tip is $PL^2/(EI) = 7.0$. The exact linear solution of the vertical tip deflection of the cantilever beam is given by Prathap and Bhashyam (1982) as

$$w_r = \frac{PL^3}{3EI}\left(1 + \frac{3EI}{k\mu AL^2}\right) \tag{84}$$

For the comparison in the following examples, the rod element including the shear deformation is denoted as 'TKREM', the rod element not including the shear deformation (Cai, Paik and Atluri 2009b) is denoted as 'TNREM', the rod element including the shear deformation and based on the primal principle (Zhu, Cai, Paik and Atluri 2010) is denoted as 'TKRE', and the two nodal Timoshenko shear flexible beam element with reduced integration is denoted as 'TSBE'.

Tab.1 shows the comparison of the deflection at the tip for the linear analysis for different ratios of h/L. Tab.2 shows the comparison of the deflection at the tip for the large deformation analysis for different ratios of h/L.

Table 1: Comparison of the deflection (δ/L) at the tip for linear analysis

h/L	0.4	0.2	0.1	0.05	0.02	0.001	0.0001
TNREM	2.33400	2.33300	2.33350	2.33325	2.33330	2.33334	2.33333
TKREM	2.67400	2.41800	2.35450	2.33875	2.33420	2.33334	2.33333
TKRE	2.67400	2.41800	2.35450	2.33875	2.33420	2.33334	2.33333
TSBE	2.67800	2.41500	2.34950	2.33300	2.32840	2.32750	2.32750
Exact	2.67000	2.41700	2.35450	2.33850	2.33420	2.33334	2.33333

The results presented in Tab.1 indicate that the present element TKREM has very good characteristics of being free from locking for linear analysis of a rod.

It is shown in Tab.2 that, except for the shear strain, the Poisson's ration has a little influence to the results of the large deformation analysis of rod (for different ratios of h/L). Tab.2 also indicates that the accuracy of the present element is comparable to the element based on primal principle, although the simple linear trial function approaches are used here.

Table 2: Comparison of the deflection(δ/L) at the tip for nonlinear analysis

h/L	0.4	0.2	0.1	0.05	0.02	0.001	0.0001
TNREM	0.85800	0.79900	0.78500	0.78150	0.78060	0.78045	0.78045
TKREM	0.92600	0.81700	0.78950	0.78275	0.78080	0.78045	0.78045
TKRE	0.89800	0.81100	0.78800	0.78225	0.78070	0.78042	0.78042

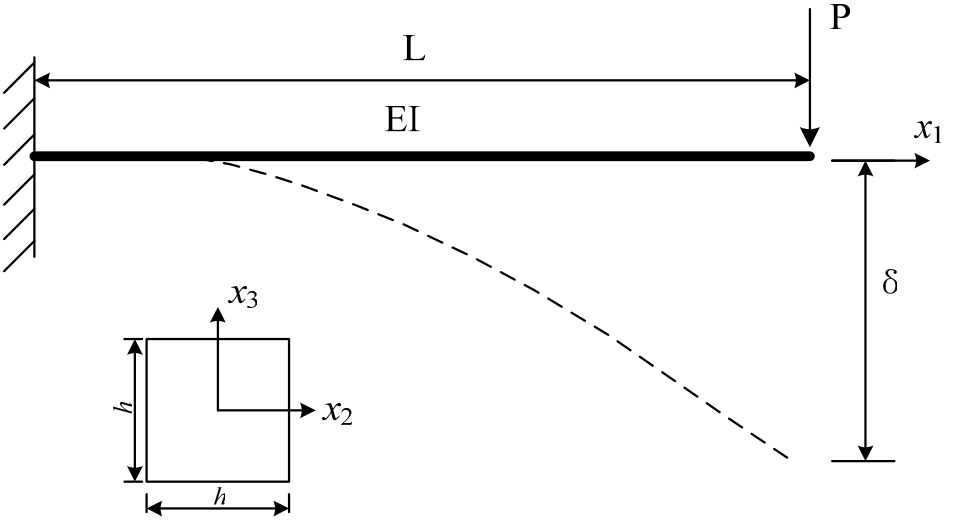

Figure 3: A cantilever beam subject to a transverse load at the tip

5.2 A cantilever beam with an asymmetric cross section

We consider a cantilever beam with an asymmetric cross section, as shown in Fig.4. The Poisson's ration is $\nu = 0.3$. The areas of cross section in Fig.4 are $A = 1$. The transverse load at the tip is $PL^2/(EI_{33}) = 7.0$. Let $h = A^{1/2}$ be the characteristic length of the cross section.

Tab.3 shows the comparison of the deflection u_2/L at the tip for linear analysis for different ratios of h/L. Tab.4 shows the comparison of the deflection u_3/L at the

Table 3: Comparison of the deflection (u_2/L) at the tip for linear analysis

h/L	0.4	0.2	0.1	0.05	0.02	0.001	0.0001
TNREM	3.24400	3.24400	3.24450	3.24425	3.24430	3.24432	3.24450
TKREM	2.53800	3.06800	3.20000	3.23325	3.24250	3.24431	3.24450
TKRE	2.54400	3.06300	3.19300	3.22575	3.23480	3.23655	3.23650

tip for linear analysis for different ratios of h/L.

Table 4: Comparison of the deflection (u_3/L) at the tip for linear analysis

h/L	0.4	0.2	0.1	0.05	0.02	0.001	0.0001
TNREM	5.44800	5.44900	5.44900	5.44875	5.44880	5.44883	5.44900
TKREM	8.94400	6.32300	5.66750	5.50350	5.45760	5.44886	5.44900
TKRE	8.92200	6.31100	5.65850	5.49550	5.44980	5.44109	5.44100

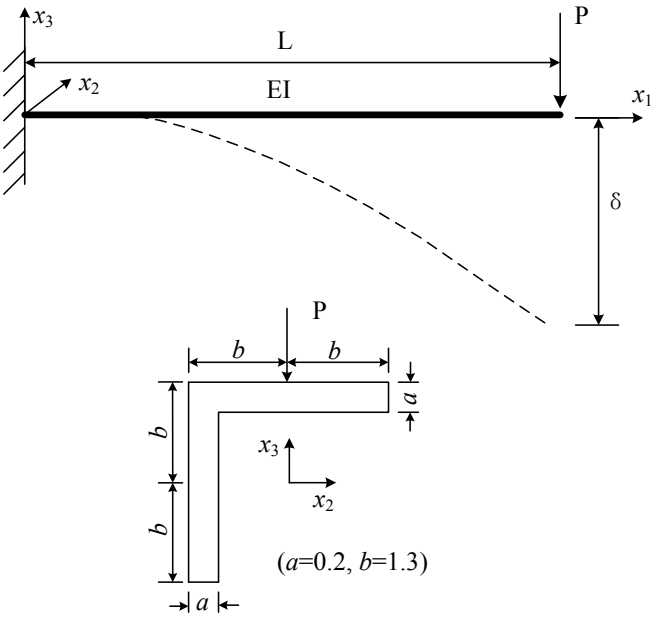

Figure 4: A cantilever beam with an asymmetric cross section

Fig.5 shows the comparison of the deflections in x_3 direction for the cantilever beam

with asymmetric cross section by using different rod elements, when $h/L = 0.1$. Fig.6 shows the deflection in x_2 direction for the cantilever beam with asymmetric cross section by using different rod elements, when $h/L = 0.1$. It is noted that the scale of the abscissa axis should be corrected to $P/2500$ and $E = 0.75e8$ in the same cantilever example with asymmetric cross section in Cai, Paik and Atluri (2009a, b).

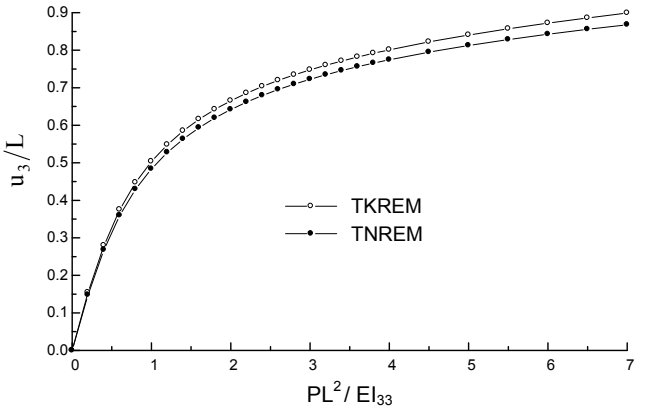

Figure 5: Comparison of the deflections in x_3 direction for the cantilever beam with asymmetric cross section

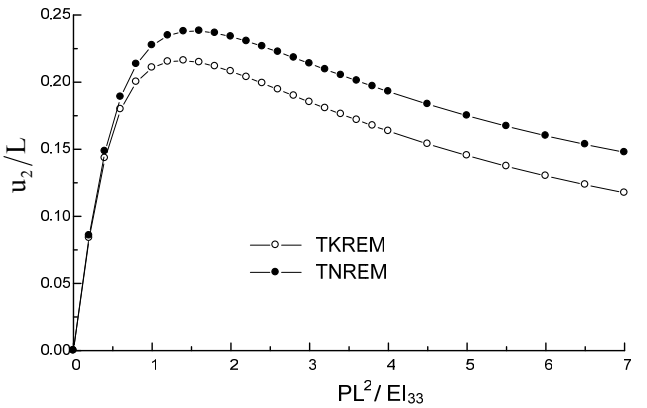

Figure 6: Deflections in x_2 direction for the cantilever beam with asymmetric cross section

5.3 Large rotations of a cantilever subject to an end-moment and a transverse load

An initially-straight cantilever subject to an end moment $M^* = \frac{ML}{2\pi EI}$ (Crisfield 1990) as shown in Fig.7, is considered. The cross section of the beam is the same as the Fig.3. The beam is divided into 10 equal elements. Fig.6 shows the comparison of the deflections in x_3 direction for the cantilever beam by using the thin/thick beam elements, when $h/L = 0.1$.

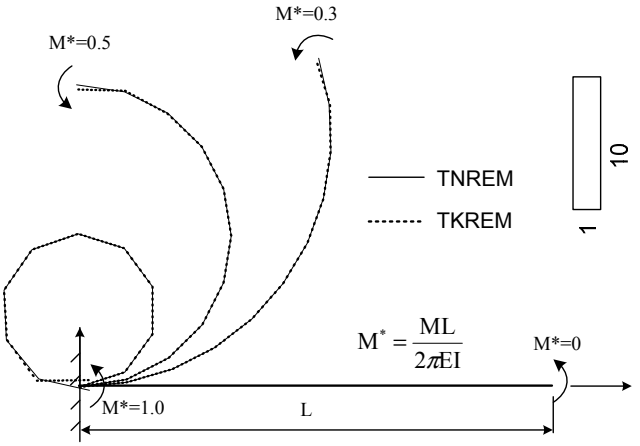

Figure 7: Initial and deformed geometries for cantilever subject to an end-moment by using the thin/thick beam elements ($h/L = 0.1$)

If a non-conservative, follower-type transverse load $P^* = \frac{PL^2}{2\pi EI}$ is applied at the tip, instead of M^*, the comparison of the deflections in x_3 direction for the cantilever beam by using the thin/thick beam elements, when $h/L = 0.2$, is shown in Fig.8.

5.4 A framed dome

A framed dome shown in Fig.9 is considered (Shi and Atluri 1988). A concentrated vertical load P is applied at the crown point. Each member of the dome is modeled by 4 elements. The comparison of the deflections in x_3 direction at the crown point by using the thin/thick beam elements is shown in Fig.10.

6 Conclusions

Based on the Reissner variational principle and a von Karman type nonlinear theory of deformation, a new shear flexible rod/beam element has been developed for

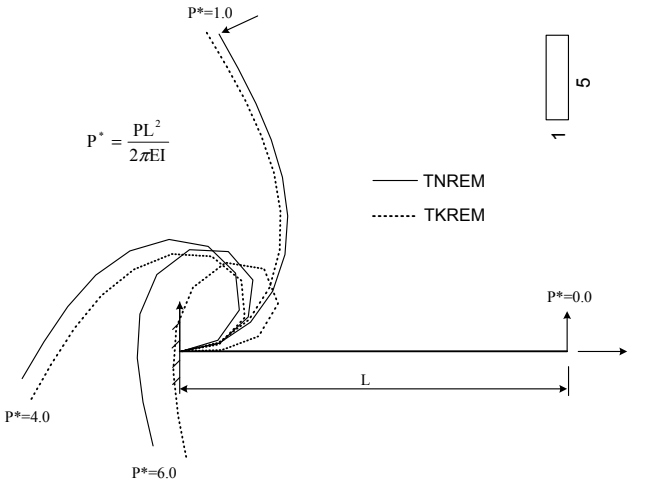

Figure 8: Initial and deformed geometries for cantilever subject to a transverse load by using the thin/thick beam elements ($h/L = 0.2$)

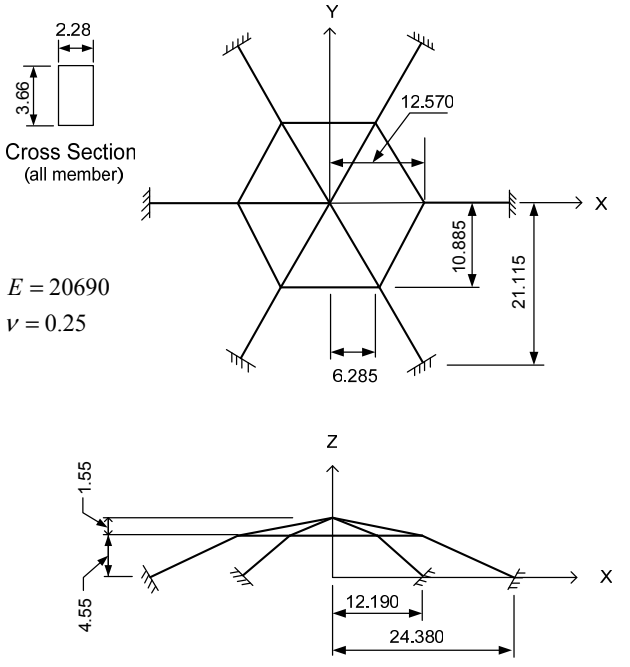

Figure 9: Framed dome

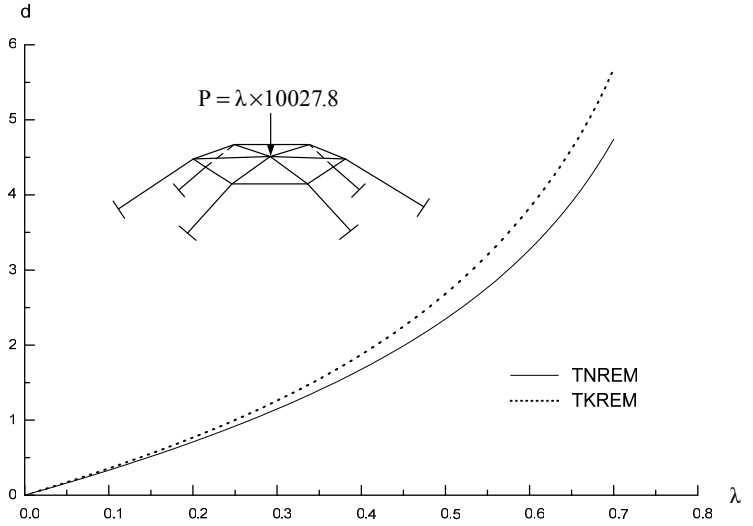

Figure 10: The comparison of the deflections in x_3 direction for the crown point of a framed dome

large deformation analysis of space frames. The trial functions for the derivatives of transverse displacements, the bending moments, the shear forces, and the torque, all can be simply assumed to be linear within each element in the current approach. Thus the development of the present element based on the Reissner's principle is much simpler than the thick-thin element based on the primal method presented in Zhu, Cai, Paik and Atluri (2010). This simplicity will become much more pronounced when the present development is extended, as planned, to plate and shell elements. The explicit expressions for the (16x16) tangent stiffness matrix of each element can be seen to be derived as text-book examples of nonlinear analyses. Numerical examples demonstrate that the present method is just as competitive as the existing methods in terms of accuracy and efficiency. The present method can be extended to consider the formation of plastic hinges in each beam of the frame; and also to consider large-rotations of plates and shells.

Acknowledgement: The authors gratefully acknowledge the support of Kwang-Hua Fund for College of Civil Engineering, Tongji University. This research was also supported by the World Class University (WCU) program through the National Research Foundation of Korea funded by the Ministry of Education, Science and Technology (Grant no.: R33-10049). The second author is also pleased to acknowledge the support of The Lloyd's Register Educational Trust (The LRET)

which is an independent charity working to achieve advances in transportation, science, engineering and technology education, training and research worldwide for the benefit of all.

References

Atluri, S.N. (1975): On 'hybrid' finite element models in solid mechanics, Advances in computer methods for partial differential equations, R. Vichrevetsky, Ed., AICA, pp. 346-355.

Atluri, S.N. (1979): On rate principles for finite strain analysis of elastic and inelastic nonlinear solids, Recent research on mechanical behavior, University of Tokyo Press, pp. 79-107.

Atluri, S.N. (1980): On some new general and complementary energy theorems for the rate problems in finite strain, classical elastoplasticity. *Journal of Structural Mechanics*, Vol. 8(1), pp. 61-92.

Atluri, S.N. (1984): Alternate stress and conjugate strain measures, and mixed variational formulations involving rigid rotations, for computational analyses of finitely deformed plates and shells: part-I: thoery. *Computers & Structures*, Vol. 18(1), pp. 93-116.

Atluri, S.N. (2005): Methods of Computer Modeling in Engineering & Science. Tech Science Press.

Atluri, S.N.; Cazzani, A. (1994): Rotations in computational solid mechanics, invited feature article. *Archives for Computational Methods in Engg.*, ICNME, Barcelona, Spain, Vol 2(1), pp. 49-138.

Atluri, S.N.; Cho, J.Y.; Kim, H.G. (1999): Analysis of thin beams, using the meshless local Petrov-Galerkin method, with generalized moving least squares interpolations. *Computational Mechanics*, Vol 24, pp. 334-347.

Atluri, S.N.; Gallagher, R.H.; Zienkiewicz, O.C. (Editors). (1983): Hybrid & Mixed Finite Element Methods, J. Wiley & Sons, 600 pages.

Atluri, S.N.; Iura, M.; Vasudevan, S. (2001): A consistent theory of finite stretches and finite rotations, in space-curved beams of arbitrary cross-section. *Computational Mechanics*, vol.27, pp.271-281

Atluri, S.N.; Murakawa, H. (1977): On hybrid finite element models in nonlinear solid mechanics, finite elements in nonlinear mechanics, P.G. Bergan et al, Eds., Tapir Press, Norway, vol. 1, pp. 3-40.

Atluri, S.N.; Reissner, E. (1989): On the formulation of variational theorems involving volume constraints. *Computational Mechanics*, vol. 5, pp 337-344.

Atluri, S.N.; Zhu, T. (1998): A new Meshless Local Petrov-Galerkin (MLPG)

approach in computational mechanics. *Computational Mechanics*, vol.22, pp.117-127

Auricchio, F.; Carotenuto, P.; Reali, A. (2008): On the geometrically exact beam model: A consistent, effective and simple derivation from three-dimensional finite-elasticity. *International Journal of Solids and Structures*, vol.45, pp. 4766–4781.

Bathe, K.J.; Bolourchi, S. (1979): Large displacement analysis of three- dimensional beam structures. *International Journal for Numerical Methods in Engineering,* vol.14, pp.961-986.

Cai, Y.C.; Paik, J.K.; Atluri S.N. (2009a): Large deformation analyses of space-frame structures, with members of arbitrary cross-section, using explicit tangent stiffness matrices, based on a von Karman type nonlinear theory in rotated reference frames. *CMES: Computer Modeling in Engineering & Sciences*, vol. 53, pp.123-152.

Cai, Y.C.; Paik, J.K.; Atluri S.N. (2009b): Large deformation analyses of space-frame structures, using explicit tangent stiffness matrices, based on the Reissner variational principle and a von Karman type nonlinear theory in rotated reference frames. *CMES: Computer Modeling in Engineering & Sciences*, vol. 54, pp.335-368.

Chan, S.L. (1996): Large deflection dynamic analysis of space frames. *Computers & Structures*, vol. 58, pp.381-387.

Crisfield, M.A. (1990): A consistent co-rotational formulation for non-linear, three-dimensional, beam-elements. *Computer Methods in Applied Mechanics and Engineering*, vol.81, pp. 131–150.

Dinis, L.W.J.S.; Jorge, R.M.N.; Belinha, J. (2009): Large deformation applications with the radial natural neighbours interpolators. *CMES: Computer Modeling in Engineering & Sciences*, vol.44, pp. 1-34

Gato, C.; Shie, Y. (2008): Numerical Simulations of Dynamic Fracture in Thin Shell Structures. *CMES: Computer Modeling in Engineering & Sciences*, Vol.33, pp. 269-292.

Gendy, A.S.; Saleeb, A.F. (1992): On the finite element analysis of the spatial response of curved beams with arbitrary thin-walled sections. *Computers & Structures*, vol.44, pp.639-652

Han, Z.D.; Rajendran, A.M.; Atluri, S.N. (2005): Meshless Local Petrov- Galerkin (MLPG) approaches for solving nonlinear problems with large deformations and rotations. *CMES:Computer Modeling in Engineering & Sciences*, vol.10, pp. 1-12

Iura, M.; Atluri, S.N. (1988): Dynamic analysis of finitely stretched and rotated 3-dimensional space-curved beams. *Computers & Structures*, Vol. 29, pp.875-889

Izzuddin, B.A. (2001): Conceptual issues in geometrically nonlinear analysis of 3D framed structures. *Computer Methods in Applied Mechanics and Engineering*, vol.191, pp. 1029–1053.

Kondoh, K.; Tanaka, K.; Atluri, S.N. (1986): An explict expression for the tangent-stiffness of a finitely deformed 3-D beam and its use in the analysis of space frames. *Computers & Structures*, vol.24, pp.253-271.

Kondoh, K.; Atluri, S.N. (1987): Large-deformation, elasto-plastic analysis of frames under nonconservative loading, using explicitly derived tangent stiffnesses based on assumed stresses. *Computational Mechanics*, vol.2, pp.1-25.

Kulikov, G.M.; Plotnikova, S.V. (2008): Finite rotation geometrically exact four-node solid-shell element with seven displacement degrees of freedom. *CMES: Computer Modeling in Engineering & Sciences*, Vol.28, pp. 15-38.

Lee, M.H.; Chen, W.H. (2009): A three-dimensional meshless scheme with background grid for electrostatic-structural analysis. *CMC:Computers Materials & Continua*, vol.11, pp. 59-77.

Lee, S.Y.; Lin, S.M.; Lee, C.S.; Lu, S.Y.; Liu, Y.T. (2008): Exact large deflection of beams with nonlinear boundary conditions.*CMES: Computer Modeling in Engineering & Sciences*, vol.30, pp. 27-36.

Lee, S.Y.; Lu, S.Y.; Liu, Y.R.; Huang, H.C. (2008): Exact large deflection solutions for Timoshenko beams with nonlinear boundary conditions. *CMES: Computer Modeling in Engineering & Sciences*, vol.33, pp. 293-312.

Lee, S.Y.; Wu, J.S. (2009): Exact Solutions for the Free Vibration of Extensional Curved Non-uniform Timoshenko Beams. *CMES:Computer Modeling in Engineering & Sciences*, vol.40, pp.133-154.

Li, Z.X. (2007): A mixed co-rotational formulation of 2D beam element using vectorial rotational variables. *Communications in Numerical Methods in Engineering*, Vol.23, pp.45–69.

Liu, C. S. (2007a): A modified Trefftz method for two-dimensional Laplace equation considering the domain's characteristic length. *CMES:Computer Modeling in Engineering & Sciences*, vol. 21, pp. 53-66.

Liu, C.S. (2007b): A highly accurate solver for the mixed-boundary potential problem and singular problem in arbitrary plane domain. *CMES:Computer Modeling in Engineering & Sciences*, vol. 20, pp. 111-122.

Liu, C.S.; Atluri, S.N. (2008): A novel time integration method for solving a large system of non-linear algebraic equations. *CMES:Computer Modeling in Engineering & Sciences*, vol.31, pp. 71-83.

Lo, S.H. (1992): Geometrically nonlinear formulation of 3D finite strain beam

element with large rotations. *Computers & Structures*, vol.44, pp.147-157

Majorana, C.E.; Salomoni, V.A. (2008): Dynamic Nonlinear Material Behaviour of Thin Shells in Finite Displacements and Rotations. *CMES: Computer Modeling in Engineering & Sciences*, Vol.33, pp. 49-84.

Mata, P.; Oller, S.; Barbat A.H. (2007): Static analysis of beam structures under nonlinear geometric and constitutive behavior. *Computer Methods in Applied Mechanics and Engineering*, vol.196, pp. 4458–4478.

Mata, P.; Oller, S.; Barbat A.H. (2008): Dynamic analysis of beam structures considering geometric and constitutive nonlinearity. *Computer Methods in Applied Mechanics and Engineering*, vol.197, pp. 857–878.

Mukherjee, S.; Prathap G. (2001): Analysis of shear locking in Timoshenko beam elements using the function space approach. *Communications in Numerical Methods in Engineering*, Vol.17, pp. 385–393.

Prathap, G.; Bhashyam, G.R. (1982): Reduced integration and the shear-flexible beam element. *International Journal for Numerical Methods in Engineering,* vol.18, pp.195-210.

Punch, E.F.; Atluri, S.N. (1984): Development and testing of stable, invariant, isoparametric curvilinear 2-D and 3-D hybrid-stress elements. *Computer Methods in Applied Mechanics and Engineering*, Vol.47, pp.331-356

Rabczuk, T.; Areias, P. (2006): A meshfree thin shell for arbitrary evolving cracks based on an extrinsic basis. *CMES: Computer Modeling in Engineering & Sciences*, vol.16, pp.115-130.

Reddy, J.N.(1997): On locking-free shear deformable beam finite elements. *Computer Methods in Applied Mechanics and Engineering*, Vol.149, pp.113-132

Reissner, E. (1953): On a variational theorem for finite elastic deformations, *Journal of Mathematics & Physics*, vol. 32, pp. 129-135.

Shaw, A.; Roy, D. (2007): A novel form of reproducing kernel interpolation method with applications to nonlinear mechanics. *CMES: Computer Modeling in Engineering & Sciences*,vol.19, pp.69-98.

Simo, J.C. (1985): A finite strain beam formulation. The three-dimensional dynamic problem. Part I. *Computer Methods in Applied Mechanics and Engineering*, vol. 49, pp.55–70.

Shi, G.; Atluri, S.N. (1988): Elasto-plastic large deformation analysis of space-frames: a plastic-hinge and strss-based explict derivation of tangent stiffnesses. *International Journal for Numerical Methods in Engineering*, vol.26, pp.589-615.

Sladek, J.; Sladek, V.; Solek, P.; Atluri, S.N. (2008): Thermal analysis of Reissner-Mindlin shallow shells with FGM properties by the MLPG. *CMES: Computer Mod-*

eling in Engineering & Sciences, Vol.30, pp. 77-97.

Wen, P.H.; Hon, Y.C. (2007): Geometrically nonlinear analysis of Reissner- Mindlin plate by meshless computation. *CMES:Computer Modeling in Engineering & Sciences*, vol.21, pp.177-191.

Wu, T.Y.; Tsai, W.G.; Lee, J.J. (2009): Dynamic elastic-plastic and large deflection analyses of frame structures using motion analysis of structures. *Thin-Walled Structures*, vol.47, pp. 1177-1190.

Xue, Q.; Meek J.L. (2001): Dynamic response and instablity of frame structures. *Computer Methods in Applied Mechanics and Engineering*, vol.190, pp. 5233–5242.

Zhang, C.; Di, S. (2003): New accurate two-noded shear-flexible curved beam elements. *Computational Mechanics*, Vol.30, pp. 81-87.

Zhou, Z.H.; Chan,S.L. (2004a): Elastoplastic and Large Deflection Analysis of Steel Frames by One Element per Member. I: One Hinge along Member. *Journal of Structural Engineering*, vol. 130, pp.538–544.

Zhou, Z.H.; Chan,S.L. (2004b): Elastoplastic and Large Deflection Analysis of Steel Frames by One Element per Member. II: Three Hinges along Member. *Journal of Structural Engineering*, vol. 130, pp.545–5553.

Zhu, H.H.; Cai, Y.C.; Paik, J.K.; Atluri S.N. (2010): Locking-free thick-thin rod/beam element based on a von Karman type nonlinear theory in rotated reference frames for large deformation analyses of space-frame structures. *CMES: Computer Modeling in Engineering & Sciences*, in press.

Zhu, T.; Zhang, J.; Atluri S.N. (1999): A meshless numerical method based on the Local Boundary Integral Equation (LBIE) to solve linear and nonlinear boundary value problems. *Engineering Analysis with Boundary Elements*, vol. 23, pp.375–389.